THE PENNSYLVANIA STATE UNIVERSITY
SCHREYER HONORS COLLEGE

DEPARTMENT OF BIOENGINEERING

PARTICLE SORTING WITH SURFACE ACOUSTIC WAVES (SAW) FOR A FULLY INTEGRATED MICROFLUIDIC FLOW CYTOMETER

KARTHIK PISUPATI
SPRING 2010

A thesis
submitted in partial fulfillment
of the requirements
for a baccalaureate degree
in Bioengineering
with honors in Bioengineering

Reviewed and approved* by the following:

Tony Jun Huang
Assistant Professor of Engineering Science and Mechanics
Thesis Supervisor

William Hancock
Associate Professor of Bioengineering
Honors Adviser

Siyang Zheng
Assistant Professor of Bioengineering

* Signatures are on file in the Schreyer Honors College.

Abstract

Flow cytometry and fluorescence activated cell sorting (FACS) are powerful analytical techniques with applications in a variety of fields, but restricted to use in specialty settings. Realizing a microfluidic flow cytometer would greatly improve the accessibility of this technology, as this would make the device portable and easily mass producible. In this thesis cell sorting techniques are reviewed in the microfluidic domain and the feasibility of a surface acoustic wave (SAW) driven sorting technique is examined. Standard soft lithography techniques were used to fabricate PDMS channels and standard surface micromachining techniques were used to fabricate inter-digitated transducers (IDT) on a piezoelectric substrate for surface acoustic wave (SAW) generation. A 3-D focused flow system with focused IDT was characterized for its particle sorting abilities with microbeads, analogous to blood cells in size and density, at varying power levels from -1dBm to 0.5 dBm. The results indicated the particles displace proportionally to the applied power. Theoretical calculations about forces and particle displacement were also considered to further understand the device functionality. The device demonstrated the ability to laterally displace particles and could ultimately be used for cell sorting purpose in a fully integrated microfluidic flow cytometer.

Table of Contents

Acknowledgements

This research was supported by National Science Foundation (ECCS-0824183 and ECCS-0801922) and the Penn State Center for Nanoscale Science (MRSEC). Components of this work were conducted at the Penn State node of the NSF-funded National Nanotechnology Infrastructure Network.

The author is indebted to Xiaole Mao for his help with experimentation and discussions about all topics related to microfluidics. The author would also like to thank Xiaoyun Ding for help in fabricating the device and discussions about acoustic waves. The author would also like to acknowledge Dr. Jinjie Shi for early discussions about SAW and SAW actuated mechanisms in microfluidics. The author is also grateful to Dr. Tony Jun Huang and the PSU BioNEMS group for their support, discussions and exposing the author to the potential of MEMS/NEMS.

I. Introduction

Miniaturization of devices has long been a fascinating subject. To this day we are captivated by small laptops, shrinking cell phones and smaller processor chips. Much of the advancement in miniaturizing devices can be attributed to the progress in microfabrication and micromachining techniques. Richard Feynman's talk "There is plenty of room at the bottom" potentially catalyzed this movement[1]. In his talk Feynman asked the audience to imagine the world of possibilities that exists at the micro scale and implored scientists to find ways to manipulate objects at the micro scale. Thus the field of Micro-Electrical-Mechanical-Systems or MEMS came to be.

In the 50 years since Feynman's talk, the field of MEMS has evolved greatly. MEMS technology has contributed to a variety of fields and has become a staple in several manufacturing industries. MEMs devices have evolved greatly and can be found in everyday devices like the Apple iPhone, or the Nintendo Wii remote. MEMs devices have also contributed in the automobile industry: tire pressure sensors, airbag accelerometers and fuel injection systems. Other MEMs applications include inkjet printing, gyroscopes, microphones and sensors such as digital light processors. According to Yole Development, in 2008, the top 30 MEMs manufacturers had combined revenue upwards of 5.5 billion dollars.[2]

1.1 BioMEMS

A sub field of MEMS is BioMEMS- which seeks to apply the principle of MEMS to solving biological problems. According to Yole, there will be significant growth in the BioMEMS industry; with market values reaching 2.13 billion dollars[3]. Normally these devices incorporate microfluidic channels, however new challenges emerge in controlling the flow in the

micro region. A great deal of research has been conducted to develop micro-actuation, pumps and valves to be used in these micro devices[4]. These pumps and valves take advantage of various techniques and material properties to achieve its means. Applying some of these concepts BioMEMS devices have demonstrated applications in sensing, particle mixing, and cell detection. It has been conjectured that BioMEMS can be to medicine what microprocessors were to computers[5]. It has the potential to revolutionize medicine by altering the fields of drug delivery, point of care diagnostics, as well as altering our views on invasive surgery, monitoring various physiological systems and even implantable devices and tissue engineering.

One sub field of BioMEMS has focused on developing analytical technology at the micro scale. Currently various physical phenomenon have been utilized to achieve these devices. At the microscale, the surface area to volume ratio increases and surface forces dominate. A primary advantage of micro devices allows for small sample sizes and parallel integration for multiple analyses. DNA microarrays take advantage of these features and have experienced great commercial success[5]. Electrical forces also scale favorably at the microscale and electrophoresis devices have also been demonstrated [5]. Development of more complex analytical devices at the microscale is currently underway, but the approach has been stepwise. Rather than demonstrate the entire device, researchers have focused on demonstrating various components, which when put together would function as the analytical device. This approach has been used to develop a microfluidic flow cytometer[6].

1.2 Flow Cytometry

Flow cytometry is a powerful analytical technique normally used by biological scientists to examine various particles including cells, DNA, proteins and other biomolecules of interest. A flow cytometer is a complex device, composed of several working parts. A figure of a

fluorescence activated cell sorter, a subtype of a flow cytometer can be seen in Figure 1.2.1. Initially the sample of interest is injected into the device; usually the sample is labeled, normally this is done through a fluorescent tag. The injected sample then flows through a narrow capillary tube and is hydrodynamically focused, this is achieved by the sheath fluid which pushes the sample flow towards the channel's center. Ultimately the sample forms a single file stream and passes through a laser at the optical interrogation area. The passing particles scatter the laser light in various directions. The scattered light is detected by various optical components. Conventional flow cytometers use three points of detection: forward scattering, side scattering and fluorescence. The scattering detection information is passed onto data analysis electronics. These components then interpret the light scattering information and analyze the sample that has passed. The most advanced flow cytometers can measure as many as thirteen parameters[7].

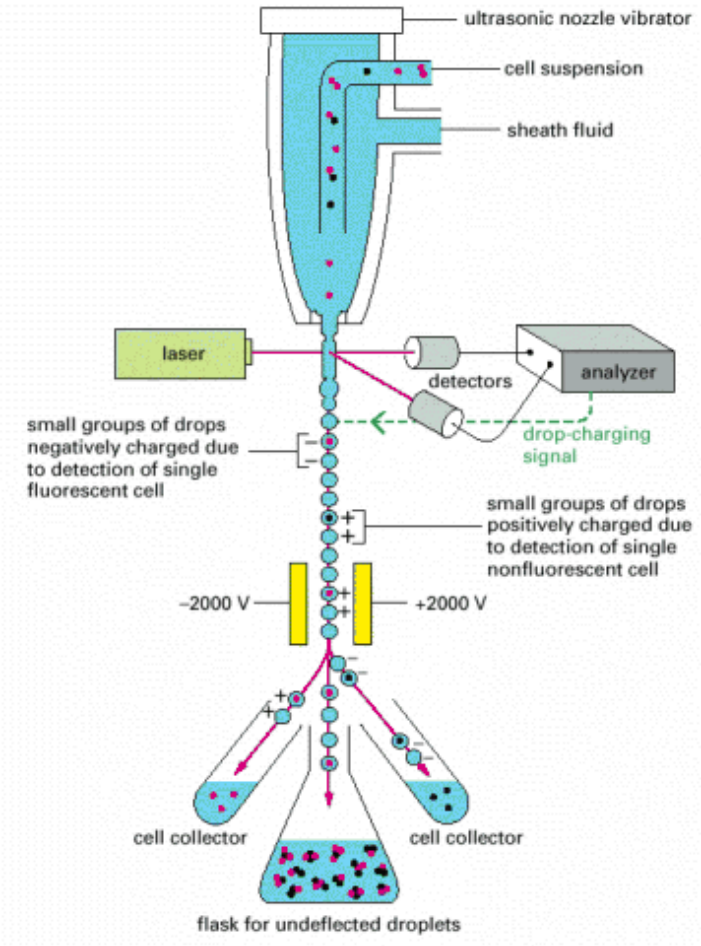

Figure 1.2.1: **Working principle of FACS**. The analyzer consists of several optical components and computer systems that analyze the sample and confer droplet charges. Source: Essential Cell Biology by Alberts.

Light scattering can provide information about important features including morphological and chemical characteristics. When used appropriately, i.e. proper staining and preparatory work, a flow cytometer can provide vital information about a cell including volume, shape, cellular contents including DNA and RNA content as well as other chemicals and proteins present in the cell[7]. This technique is not limited to cellular analysis. Flow cytometry has been modified to study smaller biomolecules including carbohydrates, protein and lipids[8]. Particles, as small as ions e.g. calcium, have also been studied with flow cytometry [7].

Flow cytometry not only provides versatility in sample analysis, but also in other potential applications. Aside from being a powerful analytical tool in cellular biology, flow cytometry has been used for diagnostics, genomics and immunology[7, 8]. Flow cytometry also can be used to sort between particles, this can be achieved by a special type of flow cytometer known as the fluorescence activated cell sorting (FACS), and an image of FACS can be seen in Figure 1.2.1. A key feature of FACS is its ability to sort between a heterogeneous sample at an extremely fast rate (10,000 particles/sec). Many commercial FACS systems resort to the stream in air sorting system to sort particles. After detection by the optical components the sample fluid flows through a nozzle. This nozzle vibrates at a specific rate determined by external systems; this vibration creates droplets at the nozzle tip as the sample fluid exits. The computer systems, which communicate with the detection systems, ensure that droplets are formed at a rate such that each droplet will likely encapsulate a single particle. The computer systems also electrically charges the droplet based on the type of particle that will be encapsulated in it. The droplets then falls through the air, hence the name stream in air, and past highly electrically charged plates (~2000 V). The charged plates create a strong electric field which deflects the droplets into the appropriate container below. The stream in air sorting system is highly efficient and despite the high voltages, particles such as cells and cellular components remain viable.

It is clear that conventional flow cytometry is an integral analytical tool in various fields. This technique not only has powerful analytical capabilities, but also offers reliable sorting methods. However these devices are expensive, large and bulky. Flow cytometers are also complex with several intertwining fluid, optical and electrical components. As a result of their complexity many of these devices require a specially trained operator. Another drawback to this

system is that it requires large sample sizes. In order to address these shortcomings, people have attempted to examine the possibility of a flow cytometer in the microfluidic domain.

As mentioned before, the strategy in developing complex microfluidic systems has been to demonstrate and optimize individual components. In this thesis, the focus is on developing a cell sorting mechanism that can sort cells on chip. Before describing the mechanism for this paper, let us examine some other techniques used to sort cells in a microfluidic channel.

II. Review of Microfluidic Sorting Techniques

Traditional FACS devices resort to charging droplets in air and using high voltages to sort cells. This method is simply not feasible at the micro-scale and other techniques have been developed to achieve the same means. A key problem in manipulating particle in the micro flow domain is the low Reynolds's number and laminar flow. These characteristic cause the particles to follow streamlines of flow, and viscous forces dominate, which make it difficult to manipulate the particles. Techniques to manipulate flow in microfluidic devices exploit various physical effects, such as hydrodynamic pressure gradients, gravity, magnetic forces, dielectrophoresis, electrokinetic flow, and optical forces[9, 10].

2.1 Pressurized hydrodynamic switching

Pressurized hydrodynamic techniques have been well explored in the microfluidic domain, primarily as a focusing technique. As mentioned hydrodynamic focusing is a vital aspect of the large scale flow cytometer because of its role in focusing the particles. This application has been translated to the microdomain and many devices incorporate a 'Y' shape or "T" shape design for sheath flow to hydrodynamically focus the main flow channel.

Several designs exist that take advantage of pressurized hydrodynamic effects to achieve flow switching. One method uses the concepts from focusing the main flow with sheath flows, but rather than focus the flow with sheath fluid, this technique uses the sheath fluid to redirect the main flow stream[11]. The schematic image for this technique can be seen below in Figure 2.1.1. The sheath flow is controlled by external pressure pumps and the particle can be sorted in a binary fashion by increasing the appropriate sheath flow. An issue with this device is that the sheath fluid must be selected appropriately, and should not contaminate the cell sample. Another

issue is that the pressures used are fairly high, and depending on channel geometry the flow field becomes turbulent and may result in unwanted effects.

Another pressure actuation method that eliminates the use of sheath fluid is the “moving wall” method[12]. The material commonly used for micro channel fabrication, PDMS, is elastic and deformable. In this design the authors fabricated a channel with air chambers on either side. By applying pressure to the air chambers, the walls of these chambers can be used to compress the main flow channel. Schematic can be seen in Figure 2.1.1. The device has three operation modes symmetric, when both structures are activated with the same pressures, asymmetric, when only one of the structures is activated and asymmetric activation, when both structures are activated but at differing conditions. The authors intended to use this pinching action form the walls pushing in to form droplets, but realized that the mechanism can be used to direct the droplets at a wide range of angles from the main flow channel. Some drawbacks to this mechanism are that it needs external high pressure actuation and the moving features maybe prone to failure with repeated use.

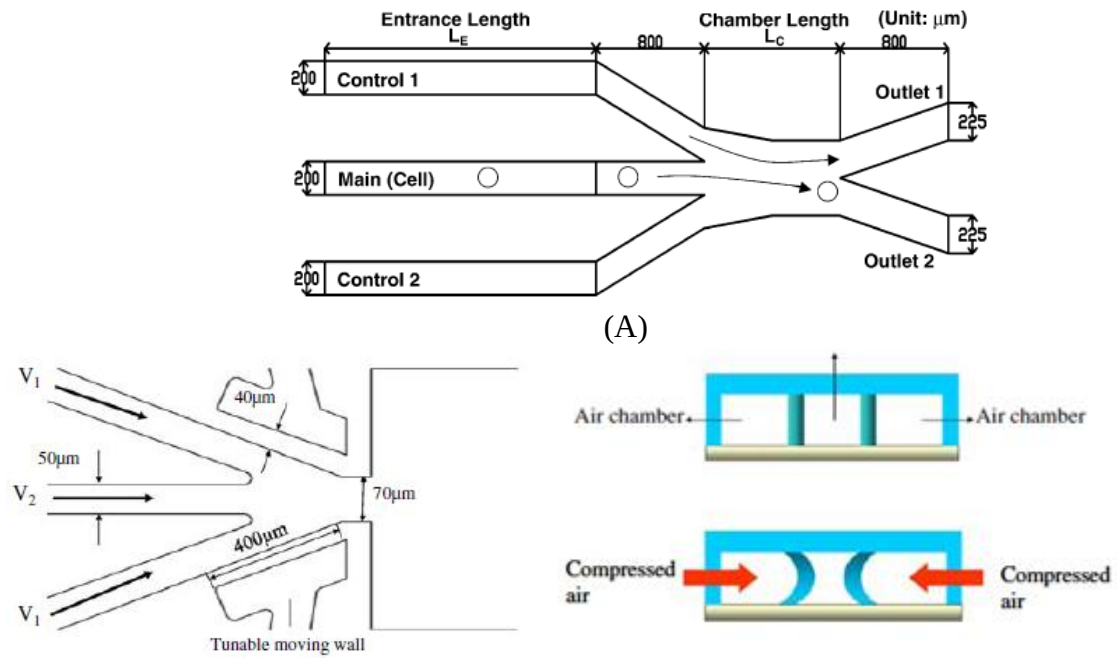

Figure 2.1.1: **Hydrodynamic switching**: (A) Using sheath flow to direct main channel flow. (B) The "moving wall" switch, where compressed air is used to change wall shape and redirect flow. Source: A is from ref. 11 and B is from ref 12.

2.2 Gravity

Another technique that has been used to sort cells in the micro-domain takes advantage of the gravitational force[13]. Huh and his group designed a microfluidic sorting device with hydrodynamic separation amplification (μ-SOHSA), which consists of a hydrodynamic focusing channel that delivers the fluid after a 90 degree turn to a widening channel, which is perpendicular to the gravitational field, that eventually leads to the collectors. The sorting principle takes advantage of the fact that denser particles tend to settle, sedimentation, as well as the geometry of the channel, which causes separation between individual streamlines as the channel widens.

This group demonstrated that their device can be used as a binary sorting system by sorting between polystyrene beads of 1 and 20 microns. By designing the upper collection

channel to be wider than the lower collection channel, the group ensured the flow rate into the upper channel to be faster than that in the lower channel. As particles approach the bifurcation region, they are directed towards the upper channel because of the bifurcation law, which states the particles will flow into the daughter channel with the higher flow rate. Since small particles tend to be towards the center of the channel and will approach the bifurcation site, these particles are directed towards faster flow in the upper channel, while larger particles will sediment and will follow the lower streamlines into the lower channel.

This device is passive and does not require external energy or controls to sort the cells. However this very quality also is a drawback as no dynamic control in sorting is presented to the user. Another consideration for gravitational sorting is that the process is dependent on flow rate. Sedimentation is a slow process and the flow rates must be maintained below a specific threshold in order for the gravitational forces to take effect.

2.3 Magnetic forces

Yet another technique used in sorting cells takes advantage of magnetic properties of particles. Magnetic forces have been extensively used in various microfluidic applications including magnetohydrodynamic (MHD) pumps, mirco-mixing with ferrofluids, particle trapping and immunoassays[14]. Particles exhibit varying magnetic properties and react differently under given magnetic conditions. This can be used to effectively sort them by applying magnetic forces.

To date many of the magnetic devices used to differentiate between cells have been continuous separators[14], meaning the particles are continually flowing and are drawn towards a magnet on the side of the channel, similar to the gravity sorting. Usually “H” shaped channels

are used and it has been demonstrated that particle can be drawn from one of channels to the other via magnets. These devices can usually sort between magnetic and non magnetic particles. Pamme et al have also demonstrated a device capable of sorting among magnetic particles by using a magnetic field gradient along the flow channel[15].

A common preparatory procedure in sorting via magnetic forces is to first label the particles with magnetic nanoparticles. Usually this is done before by incubating the particles with the magnetic nanoparticles; the amount of nanoparticles that attach are dependent upon the particle surface and the magnetic forces experienced is proportional to the number of magnetic nanoparticles attached to the surface. Some other considerations for performing magnetic separation are interactions between particle and particle aggregates. External magnet alignment also present challenges; while on chip magnet fabrication also presents challenges.

2.4 Dielectrophoresis (DEP)

Dielectrophoresis or DEP is when a neutral particle between 1 mm and 1 micrometer moves in a non-uniform electrical field because of polarization effects. DEP has also been explored extensively in microfluidics and has been demonstrated to be useful in particle separation and trapping. There are two types of DEP: positive and negative. In positive DEP the particle is attracted to the stronger electric field, while in negative DEP the particle are repelled by the stronger electric field[5].

Normally planar electrodes are easily fabricated on to the substrate before bonding a channel above. The DEP force decays exponentially with the distance from the electrodes. Holmes et al fabricated a DEP based sorter by bonding electrodes on the bottom and top of the channel to alleviate the DEP force attenuation[16]. The schematic can be seen below in Figure

2.4.1. Wang et al demonstrated a DEP sorting device, where they formed electrodes onto the sides of the flow channel[17]. The schematic of the mechanism can be seen below in Figure 2.4.1. In both case by applying the appropriate electric fields the particles in the channels can be laterally manipulated to flow into the appropriate outlet. Some considerations with DEP devices are that the system is dependent on frequency as well as the dielectric properties of the particle. So in one frequency range the particle might experience positive DEP and negative DEP at another range; knowledge of the particle's dielectric properties beforehand would vital to optimally sort it. Another consideration is cell viability under the applied voltages and frequency.

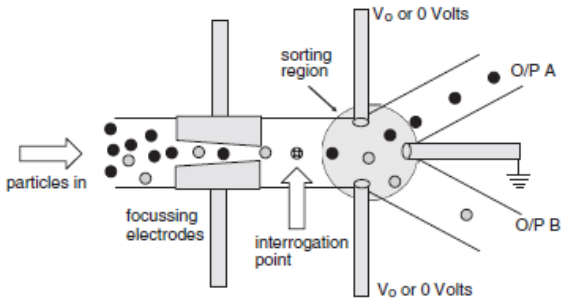

(A)

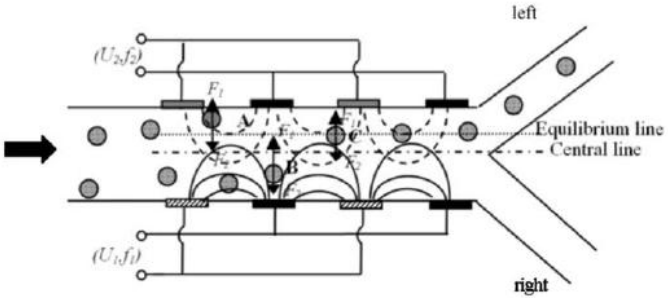

(B)

Figure 2.4.1: **DEP sorting**: (A) Bottom plane of microdevice with deposited electrodes. The same arrangement of electrodes is patterned on top of the channel. Particles are sorted by varying the voltage at the electrodes after the interrogation point. (B) Device with electrodes on sidewalls. U is voltage and *f* is frequency. Equilibrium line represents where particle will end up due to force balances. Source: A is from ref. 16 and B is from ref. 17.

2.5 Electrokinetic flow

At the microscale electrical phenomenon scale favorably and can be used to drive fluid flow. Electro-osmotic flow, also known as electrokinetic flow, occurs because an electrical double layer forms between the fluid and the channel surface. A voltage is applied to either end of the fluid channel causing the charges at the channel interfaces to migrate towards the opposite polarity. As the fluid near the walls flows, it drags the bulk fluid along with it because of viscous interactions [5].

Electrokinetic flow is widely used in microfluidics and to date two microfluidic flow cytometers, including one that is reversible, have been demonstrated[18, 19]. Both of these rely on electrokinetic driven flow not only for pumping but also cell sorting. Since the flow is determined by the polarity at the ends of the channel, the direction of the flow into one outlet over another can be controlled by applying the appropriate polarity at that outlet. Binary sorting in a T shaped channel[18] as well as flow switching between three outlets has been demonstrated. Some drawbacks to this technique are that it relies on charge carries to drive motion; this can succumb to electrical shielding effects, not to mention the flow is slower than the pressure driven counterpart. Large voltages (kV/ cm) are also applied so cell viability is a concern. The buffer fluid must also be selected carefully to prevent unwanted effects.

2.6 Optical Forces

It is evident that various avenues have been explored to manipulate particles in microfluidic flow. Optical components were largely used for detection purposes, but recently have been used to demonstrate particle manipulation[20, 21]. An image of the proposed device can be seen in Figure 2.6.1. The optical manipulation works in the sample principle as optical

tweezers. An external laser perpendicular to the fluid channel is used to trap the particle of interest in a light beam. The light beam has a working region across several stream lines. The particle is then optically coerced into the correct outlet by changing it stream line trajectory via the optical tweezers. Some considerations for this technique are the proper alignment and focus of the lasers. Since the working area for the sorting is small, proper alignment is crucial.

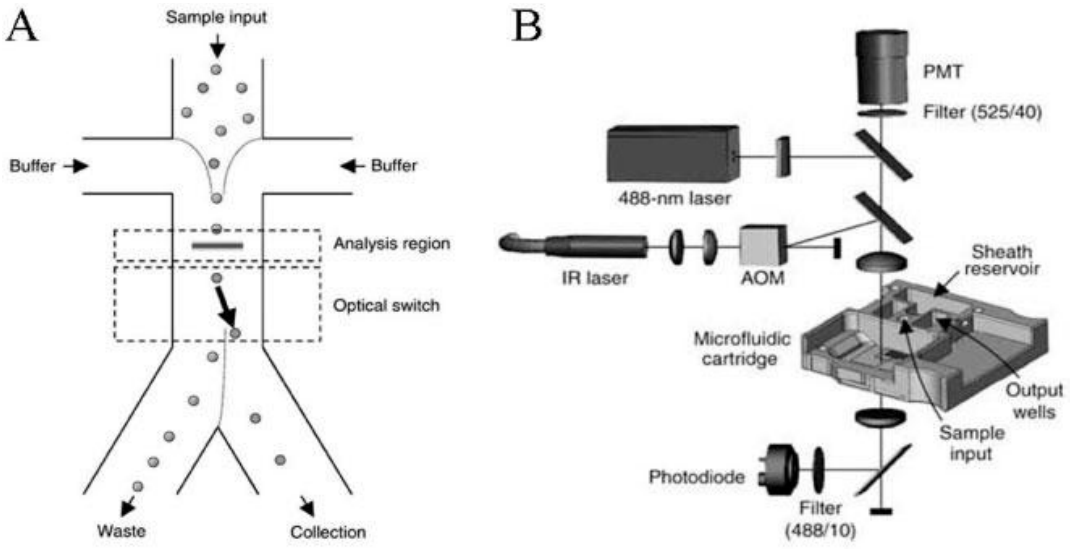

Figure 2.6.1: **Optical force switching**: (A) Schematic of device. The optical switch region acts like the optical tweezers and manipulates particles into the appropriate channel. (B) External set up for the device. Source: From ref 21.

2.7 Design idea: Acoustic Waves

Essentially every sorting technique mentioned so far has unique advantages but also potential drawbacks. An approach that uses acoustic forces to manipulate cells has not been thoroughly explored, and may provide a better alternative. Surface acoustic waves (SAWs) are pressure waves that propagate along the surface of an elastic substrate with most of the energy localized within 1~2 wavelength normal to the surface[22]. SAW have been demonstrated in various microfluidic devices including micromixers, pumping and particle focusing[23]. The energy confinement nature of SAWs makes them ideal tools for manipulating the contact

medium without interfering with the rest of the setup. In addition they consume little energy while generating large acoustics pressures, which can potentially be utilized to manipulate the contact objects, such as bio-particles.

In this thesis, the feasibility of SAW generated from a focused IDT to manipulate particles will be examined and characterized. So far droplet manipulation in bulk flow[24] and continuous flow cell separation[22] has been demonstrated. This technique when integrated with the appropriate circuitry and cell detection technology can be used to effectively to actively sort cells in a rapid manner and eventually be realized in a fully integrated flow cytometer.

III. Methods

3.1 Device Fabrication

The fabrication process was composed of several commonly used micro-device fabrication techniques of lithography and surface micromachining. The fabrication process was carried out in three basic steps: (1) the fabrication of IDTs for SAW generation; (2) the fabrication of a PDMS-based microchannel; (3) the bonding of the PDMS microchannel to the SAW substrate. The fabrication schematic can be seen in Figure 3.1.1.

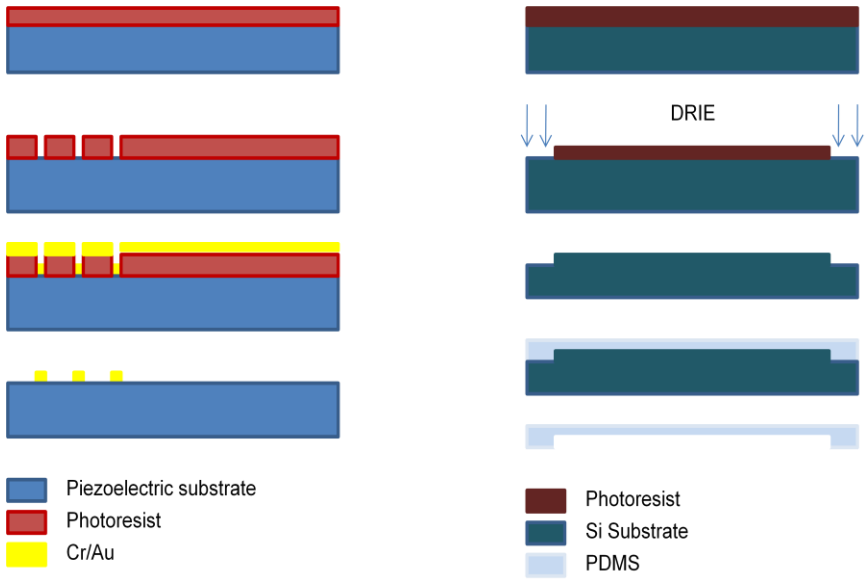

Figure 3.1.1: **Device Fabrication**: on the left is the IDT surface deposition process and on the right is the surface micromachining for the PDMS channels.

Standard metal deposition and liftoff procedures were used to fabricate the IDTs. First a photoresist layer was deposited onto the device substrate, which was 128° Y-X $LiNbO_3$, a piezoelectric material. Lithography was used to give the patterned opening of IDTs. This was followed by multilayer metal deposition for the formation of the IDT. First 50 angstrom Cr was deposited then 800 angstrom Au was deposited. The Cr acts an adhesion layer and improves the

bonding between the substrate and Au. Next the photoresist layer was lifted off, to produce the SAW substrate integrated IDTs. The wavelength of the fabricated IDT was 165 micrometers. Wires were bonded with silver conductive epoxy to the IDT electrodes to provide electrical contacts. The fabrication of the IDT device was performed at the nanofabrication facilities, by graduate student Xiaoyun Ding, who is trained in these techniques.

Next the polydimethylsiloxane (PDMS) microchannels were fabricated with standard soft-lithography and mold-replica techniques. PDMS is a commonly used material to fabricate microfluidic channels as it is easily molded and is translucent, allowing for flow visualization. The silicon mold for the microchannel was patterned by photoresist and etched by a Deep Reactive Ion Etching (DRIE) process. The mask, used in selectively etching the mold, design and the mold etching were conducted by Xiaole Mao. After DRIE, the silicon mold was coated with 1H,1H,2H,2H-perfluorooctyl-trichlorosilane (Sigma Aldrich, St. Louis, MO) in a vacuum chamber to make the extraction of PDMS channel during the demolding process less damaging. SylgardTM 184 Silicone Elastomer Base and SylgardTM 184 Silicone Elastomer Curing Agent (Dow Corning, Midland, MI) were mixed at a 10:1 (weight) ratio, and cast into the silicon mold. This mold was cured at 70 °C in an oven for 60 minutes. After peeling off the silicon mold, inlets and outlets were created using a silicon carbide drill bit.

To attach the PDMS microchannel to the substrate, both the surfaces were first activated with oxygen plasma. The alignment of the substrate and the PDMS channel were conducted manually under the microscope. Finally, polyethylene tubing was inserted into the inlets and outlets of the channel.

3.2 Experimental Methods

The fabricated channels were mounted on an inverted fluorescence microscope (TE 2000U, Nikon). The excitation light source was 488 nm. The laser beam was aligned with the center of the microfluidic channel to excite the fluorescent beads in the flow. The fluorescent emission was captured by the microscope lens. A CCD camera was used to visualize the flow pattern and to examine the sorting capabilities of SAW. Imaging software, In Vivo, was used to capture the images and image analysis was performed using Image J.

Fluorescent polystyrene microbeads of diameter 7.4 micrometers were purchased from Bangs Laboratories Inc. The beads had uniform Dragon Green fluorescence, with excitation wave length 480 nm and an emission wavelength of 520 nm. The density of the beads (1.05×10^3 kg m^{-3}) matched those of blood cells, specifically T cells (1.07×10^3 kg m^{-3})[25]. The size and density of the beads were good analogs of blood cells, making the beads good candidates to examine the feasibility of SAW driven sorting.

In the experiments, a RF signal was generated from a signal generator (Agilent E4422B) and amplified by a power amplifier (Amplifier Research 100A250A). The output signal from the amplifier was then applied to the IDT to generate SAW. The gain was set at 5 units for the various set ups. The applied AC signal was also set at a driving frequency of 24.3 MHz for the various set ups. The driving frequency can be calculated from the wavelength of the IDT (spacing between the fingers) and velocity of propagation in the substrate. Varying levels of power were used for the differing set up and were tested to characterize the displacement features of each.

A microfluidic chip with a focused IDT and 3-D focused channel was fabricated using the process mentioned earlier. A schematic of the finished device can be seen in Figure 3.2.1. The microfluidic device takes advantage of a unique design demonstrated by Mao et al for 3-D hydrodynamic focusing in a microfluidic channel[26]. This design consists of 4 inlets. Two inlets, seen in many microfluidic devices, are for sheath fluids to focus the flow horizontally in the channel. The novelty of the design is that the design uses a third sheath fluid channel along with a curved channel to focus the flow vertically in the channel. This overall design ensures a single file, focused flow, similar to the large scale FACS, passing through the interrogation region.

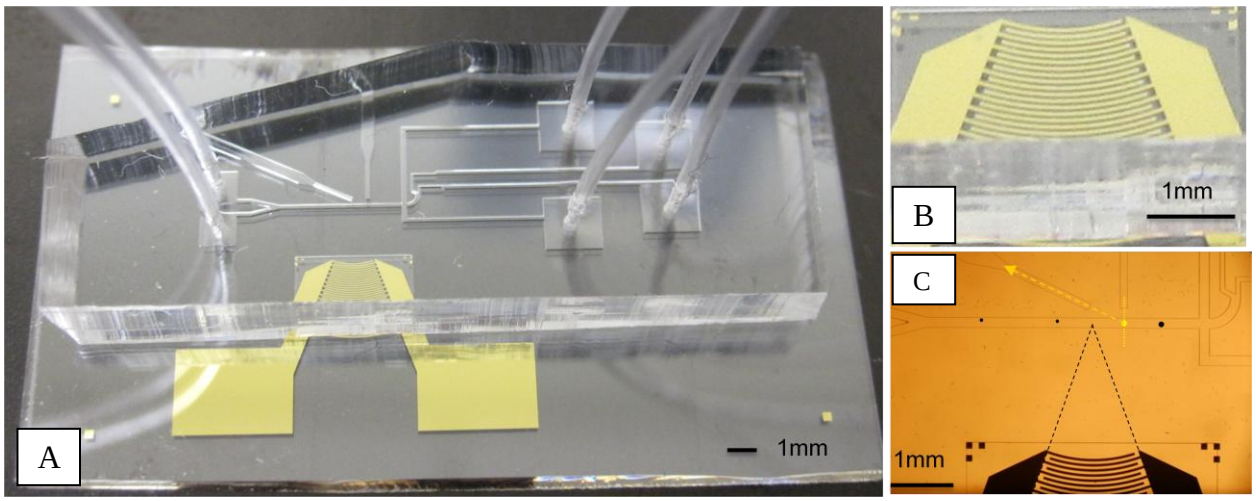

Figure 3.2.1: **Fabricated device**: (A) Picture of final fabricated microfluidic device with 4 inlets, 2 outlets, and 2 optical fiber channels. The gold is the focused IDT (B) Image of the focused IDT. The period is approximately 165 micrometers. (C) Proposed functionality of device to sort particles with focused IDT. Black dashed lines indicate hypothetical location of the focused SAW.

Syringe pumps (KD scientific) were used to inject the sample solutions. The fluorescent particles were diluted in 0.01% SDS surfactant buffer, to prevent particle aggregation, while the sheath fluids were also 0.01% SDS buffer. The flow rates were set to optimize the 3-D hydrodynamic focusing technique, which requires flow rates as high as 370 μl/min.

IV. Results

The figures in this section display the fluidic device while varying levels of power -1 dBm, -0.5 dBm and 0.5 dBm were applied. The intensity of the fluorescent particles was used as a gauge to determine lateral displacement of the particles. For each setup the upstream (before the SAW) and downstream (after the SAW) intensities was measured. The highest intensities across the channel were indicative of the fluorescent particles, and the shift in the peak position was correlated with the displacement. In each of the images from the microscope, the SAW is at the bottom of the image. The position of intensity in the channel was measured in reference to the top channel wall, i.e. the top of the channel was position 0 and the position was positive going towards the bottom channel wall, which was position 167, the channel width.

In each of the photographs, the white line traversing the middle of the channel is the stream of fluorescent particles. White spots on the edges are the particles that were bound to the channel sidewalls during the initial flow phase, before the flow rates for the 3-D hydrodynamic focusing were reached. The two rectangular geometries in each of the pictures above the main flow channel represent the optical fiber waveguides for fluorescence excitation and detection. For this study, these features were not used, but would be integrated at a later stage for a fully integrated microfluidic flow cytometer.

Image analysis was performed using Image J. Videos of the particle sorting were analyzed frame by frame. Cross section plot profiles were obtained at varying time points for each power level, while SAW was turned on and off. A minimum filter was applied to the images in order to achieve higher pixel resolutions, and sharper intensity peak, to resolve the particle positions more accurately.

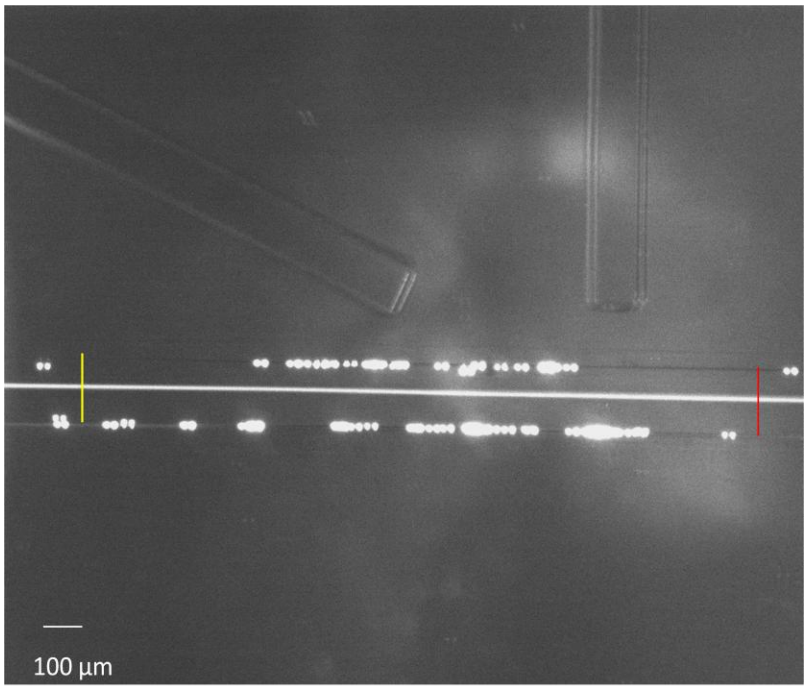

Figure 4.0.1: Image of device with SAW off at time 35 at -1 dBm applied power. The red line indicates the position from which upstream intensity was obtained and yellow line indicates the position where downstream intensities were obtained.

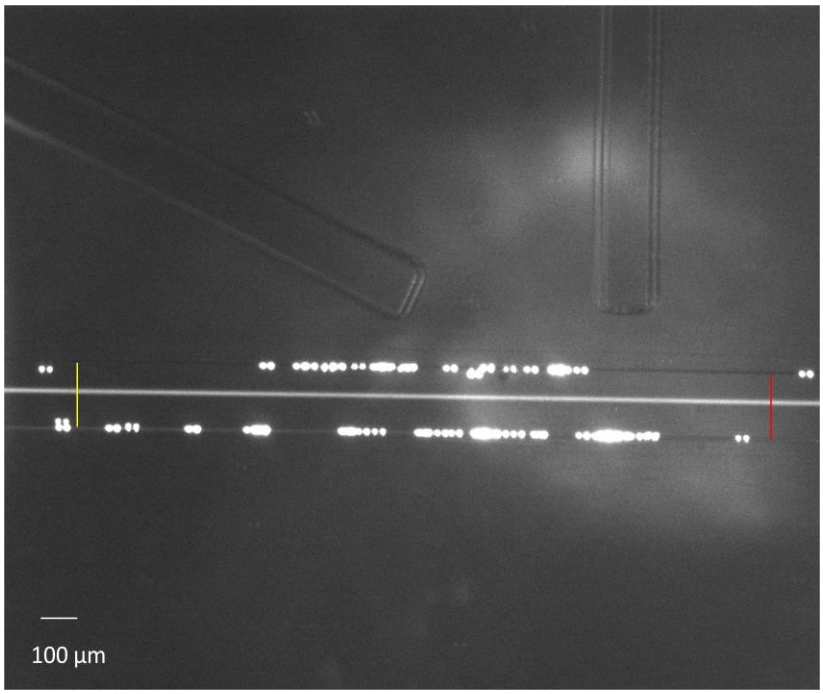

Figure 4.0.2: Image of device with SAW on at time 39 at -1 dBm applied power. The red line indicates the position from which upstream intensity was obtained and yellow line indicates the position where downstream intensities were obtained.

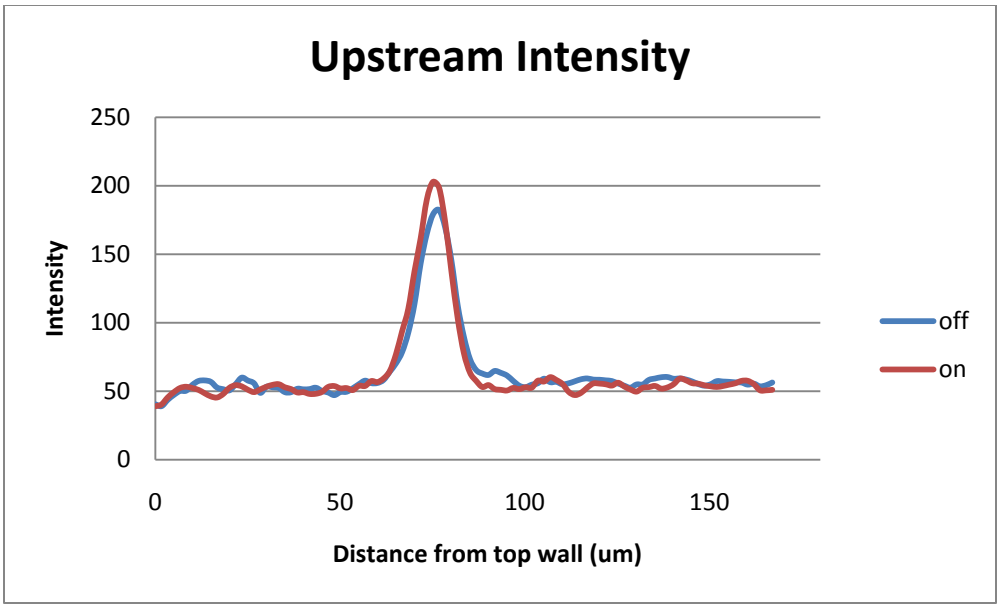

Figure 4.0.3: The upstream intensity of the particles across the channel at a power level of -1 dBm. Blue indicates while SAW is off and red is while the SAW is turned on. The peaks for both situations occur at the same position.

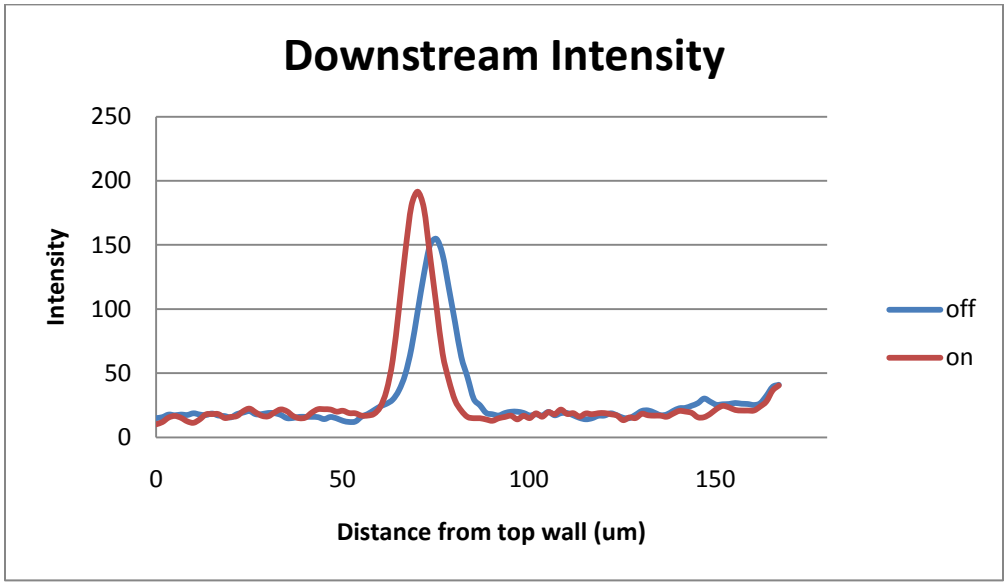

Figure 4.0.4: The downstream intensity of the particles across the channel at a power level of -1 dBm. Blue indicates while SAW is off and red is while the SAW is turned on. A clear shift in the peaks of is evident. In this case, the particle shifted approximately3.4 micrometers.

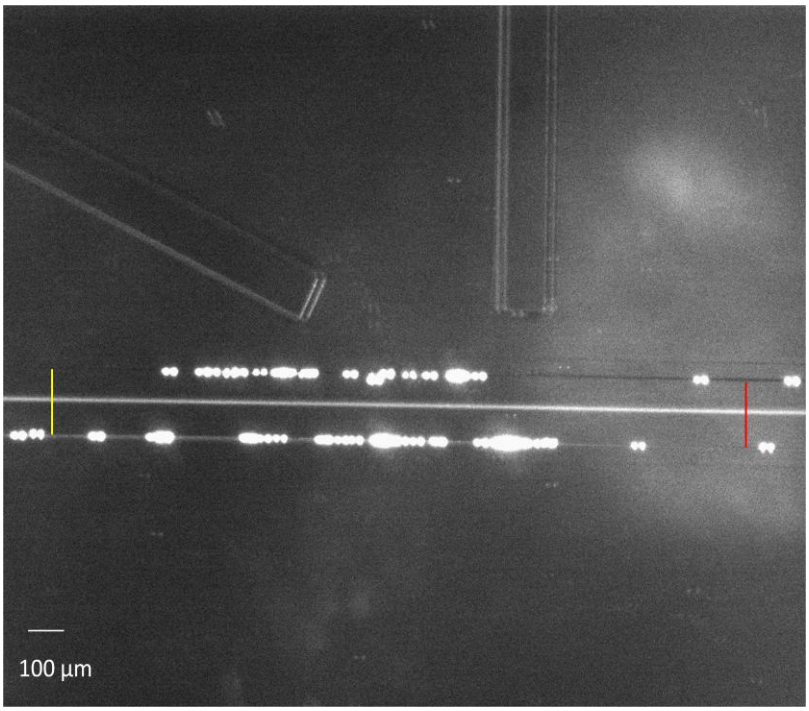

Figure 4.0.5: Image of device with SAW off at time 28 at -0.5 dBm applied power. The red line indicates the position from which upstream intensity was obtained and yellow line indicates the position where downstream intensities were obtained.

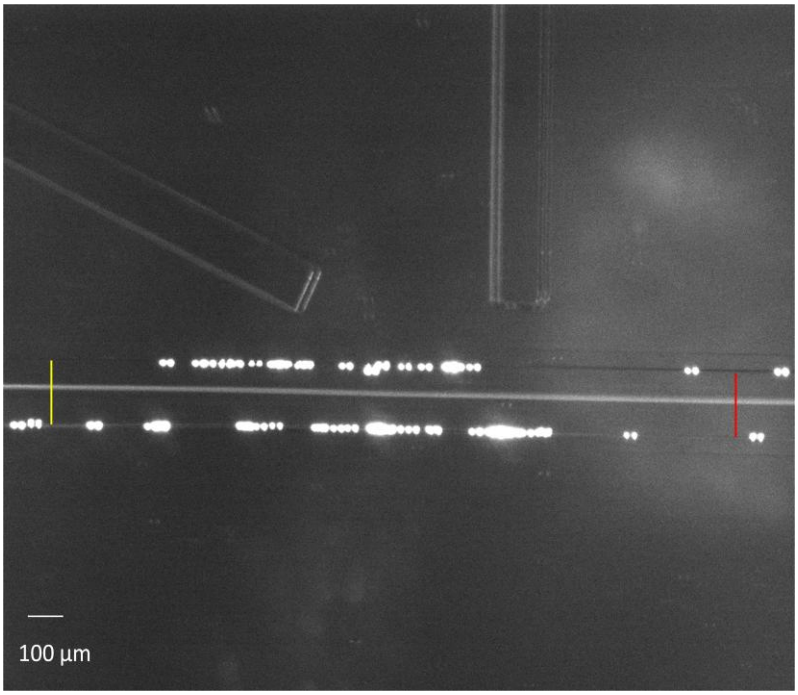

Figure 4.0.6: Image of device with SAW on at time 35 at -0.5 dBm applied power. The red line indicates the position from which upstream intensity was obtained and yellow line indicates the position where downstream intensities were obtained.

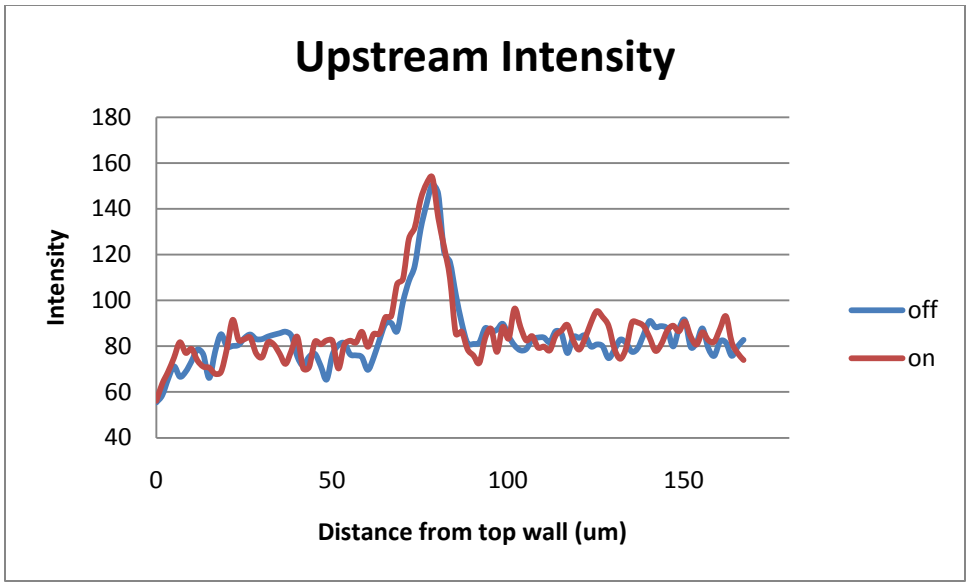

Figure 4.0.7: The upstream intensity of the particles across the channel at a power level of -0.5 dBm. Blue indicates while SAW is off and red is while the SAW is turned on. The peaks for both situations occur at relatively the same position.

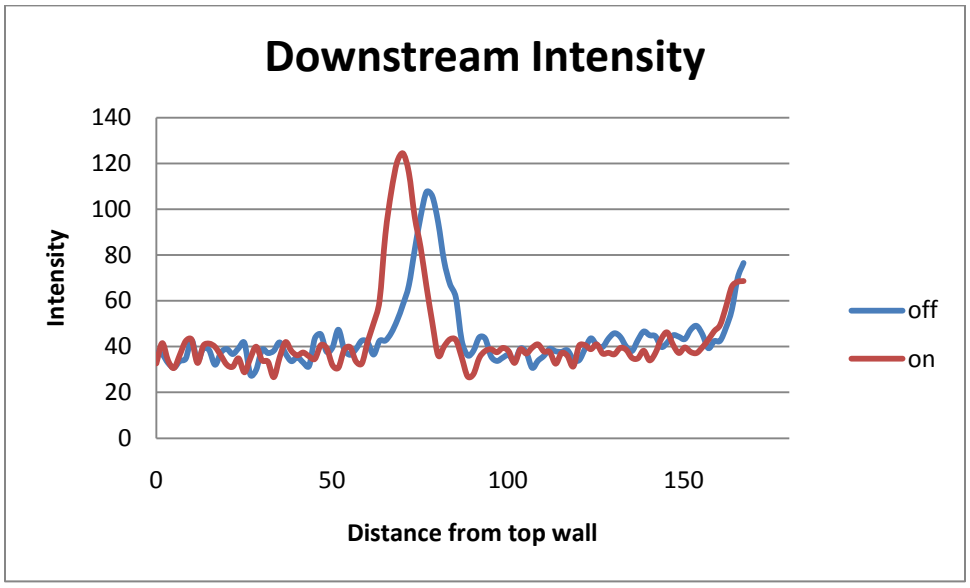

Figure 4.0.8: The downstream intensity of the particles across the channel at a power level of -0.5 dBm. Blue indicates while SAW is off and red is while the SAW is turned on. A clear shift in the peaks is evident. In this case the observed shift was 6.7 micrometers.

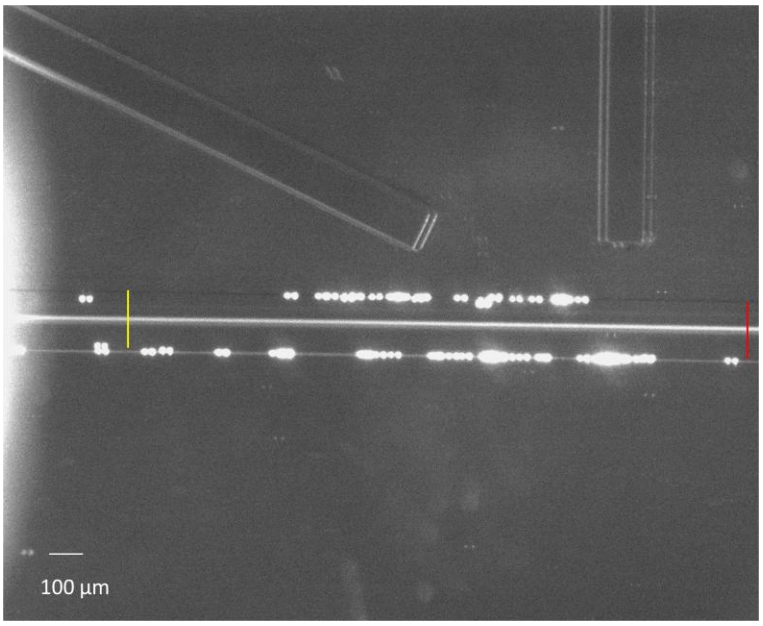

Figure 4.0.9: Image of device with SAW off at time 25 at 0.5 dBm applied power. The red line indicates the position from which upstream intensity was obtained and yellow line indicates the position where downstream intensities were obtained.

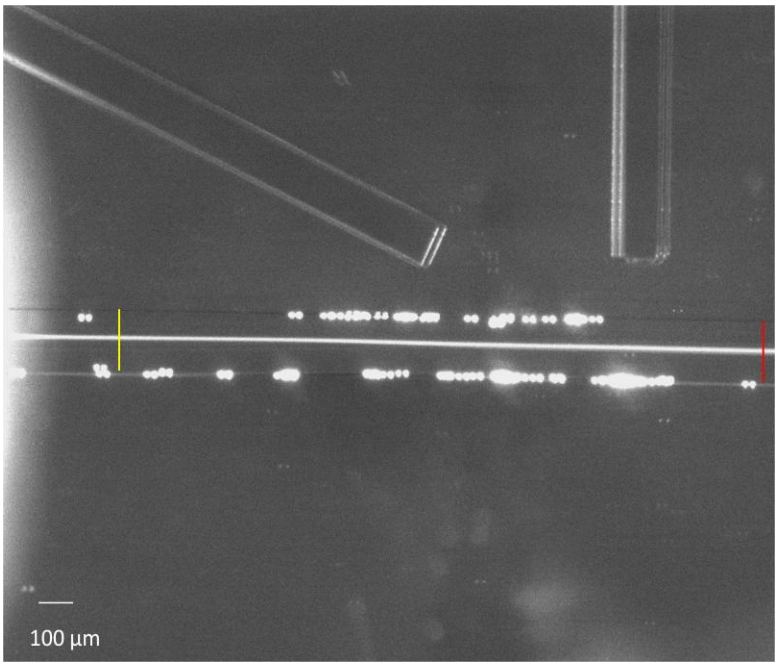

Figure 4.0.10: Image of device with SAW on at time 31 at 0.5 dBm applied power. The red line indicates the position from which upstream intensity was obtained and blue line indicates the position where downstream intensities were obtained.

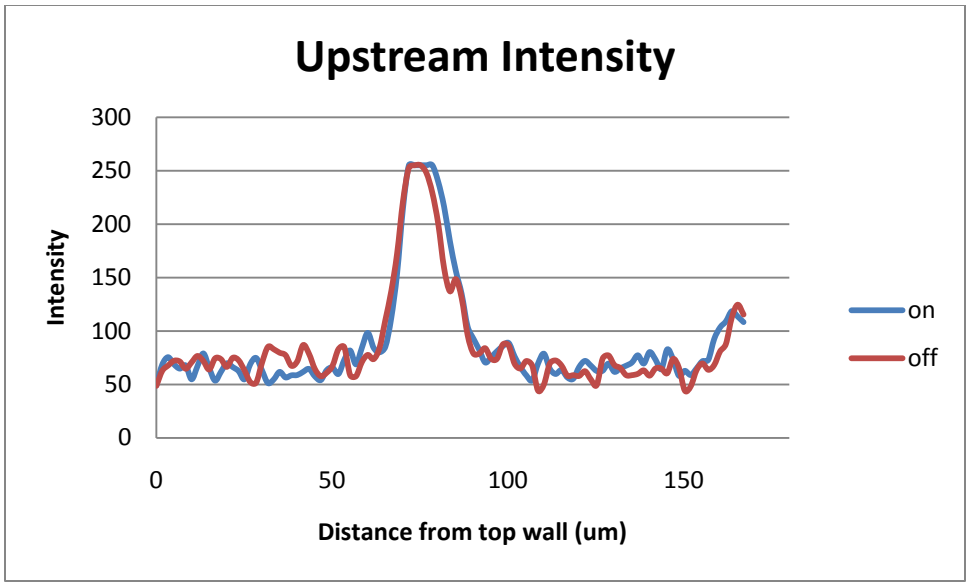

Figure 4.0.11: The upstream intensity of the particles across the channel at a power level of 0.5 dBm. Blue indicates while SAW is off and red is while the SAW is turned on. The peaks for both situations occur at the same position.

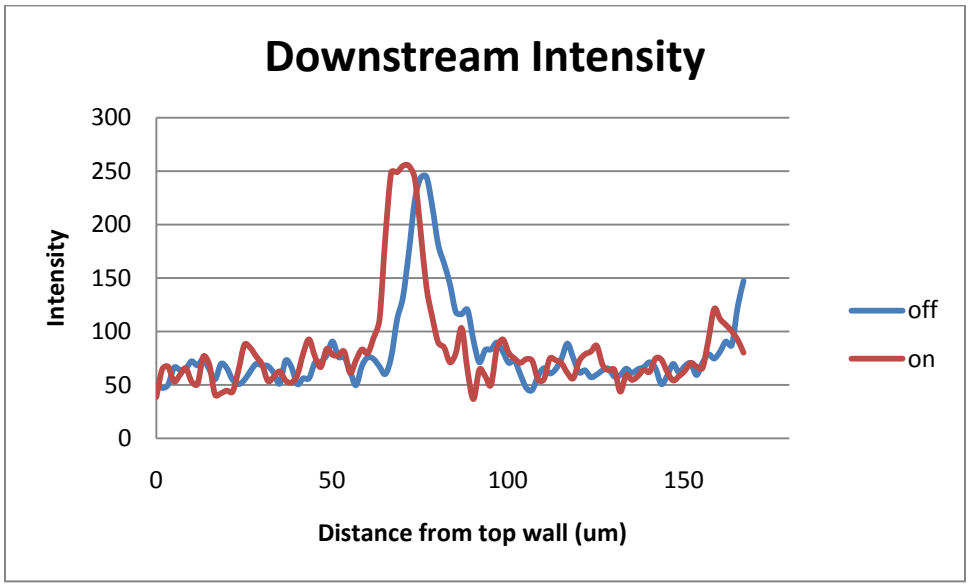

Figure 4.0.12: The downstream intensity of the particles across the channel at a power level of 0.5 dBm. Blue indicates while SAW is off and red is while the SAW is turned on. A clear shift in the peaks is evident. In this the case the observed shift was 6.7 micrometers.

In all cases the upstream intensities remained at the same position for SAW on and SAW off. This demonstrates that upstream of the SAW, the particles are not deflected. A clear shift in the peak position of the downstream intensities was observed for all cases. A summary of the applied power versus the displacement relationship can be seen below in Figure 4.0.13.

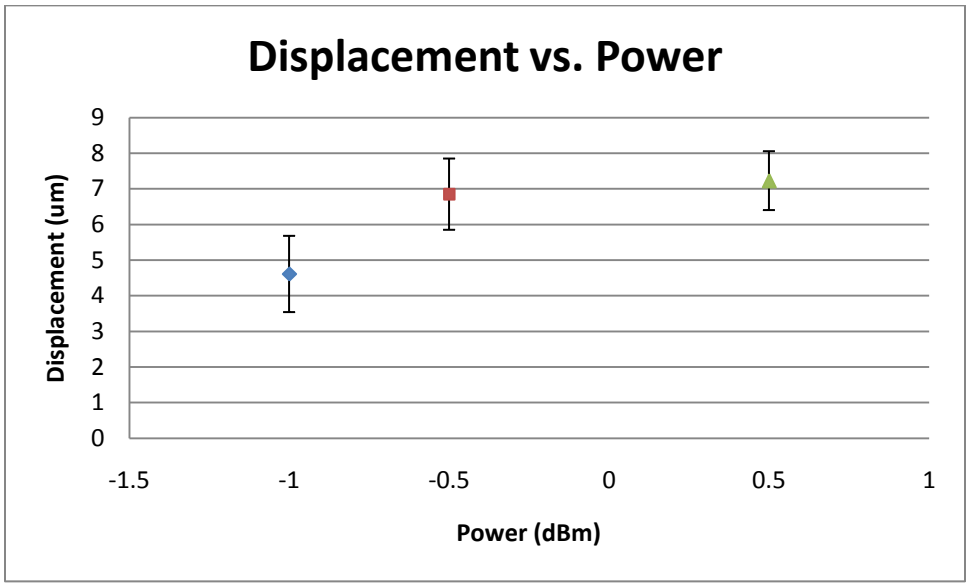

Figure 4.0.13: This shows the relationship between the displacement of the particle and the power applied. The displacement values are the mean for a given power level and the vertical error bars are the standard deviations of the displacement for various particles at the applied power.

The displacement vs. power figure indicates there is a positive relationship between power applied in dBm and the displacement. The power in dB is equivalent to 10*log of the power in milliwatts. The power values are only sampled in a narrow range as clear shifting was only observed at power levels of -1 dBm and powers exceeding 0.5 dBm would sometimes lead to cracking of the substrate. For applied power of -1 dBm the average displacement was 4.61 micrometers. For applied power of -0.5 dBm the average displacement was 6.85 micrometers and for applied power of 0.5 dBm the average displacement was 7.23 micrometers. The trend

suggested by this data is that as applied power is increased the particle displacement also increases.

In addition to the demonstrated results another phenomenon was also observed: the sidewalls of the channel would slightly deform when the SAW was applied. However, the particles in the channels would deflect well before the wall deformation suggesting this affect played a minor role, if any in displacing the particles.

V. Discussion

The laminar flow and the dominance of viscous forces in the micro flow domain present a challenge for particle manipulation. These features cause the particles to follow streamlines of flow. A surface acoustic wave (SAW) device has been developed to manipulate particles to cross stream lines and thereby achieve cell sorting at the outlet. The working mechanism of how surface acoustic waves are generated by the devices and how these waves impart forces on the particles in the channel is briefly examined below.

5.1 Working Mechanism and Theoretical analysis

Surface acoustic waves, also called Rayleigh waves because they were first described by Lord Rayleigh, are sound waves that propagate on the surface[5]. Surface acoustic waves are akin to ripples that propagate on the surface of calm water due to a disturbance. Surface acoustic waves are similarly created on the surface of the microfluidic device by creating a mechanical disturbance. Lithium Niobate ($LiNbO_3$), the substrate for the device, is a piezoelectric material. Piezoelectric materials demonstrate some unique properties: they undergo a mechanical deformation when an electrical potential is applied or they generate an electrical potential when they undergo a mechanical deformation. SAW generation takes advantage of the former effect. The indterdigitated transducers (IDT) act as electrical contacts that are used to apply a potential to the piezoelectric substrate. A radiofrequency oscillator applied at the driving frequency is used to apply the voltage to the IDT. This oscillating nature of the input signal causes one half of the fingers of the IDT to be active while the other half is inactive. The area of the substrate underneath the active finger undergoes a mechanical deformation due to the piezoelectric effect. By alternating which fingers are activated at a specific time the mechanical deformations on the surface lead to the formation of a wave that propagates through the surface. The layout of the

IDT, such as number of fingers, finger spacing, and applied power can used to alter the features of the SAW, such as the wavelength and amplitude. Geometrical changes to the shape can also alter the features of SAW. For example IDT can also be arranged in a circular fashion, an arrangement known as the focused IDT (F-IDT), is used to generate a focused acoustic wave, with a small working area in the fluid. This arrangement of F-IDT can result in higher amplitude waves and lead to greater particle displacement profiles; however second order effects such as diffraction and beam steering result in propagation losses[27].

The SAW generated by the IDT is a bidirectional wave that propagates in both the x (parallel to the surface) and z (into the substrate) directions. See Figure 5.1.1 below for schematic of SAW propagation. The surface parallel and normal components lead to the formation of an elliptical path that the wave and any particle on the surface will follow. However the energy of the SAW is localized on the surface of the substrate so the depth of penetration is shallow. This feature of SAW makes it sensitive to surface effects has made it a popular mechanism for detecting surface modulations [28].

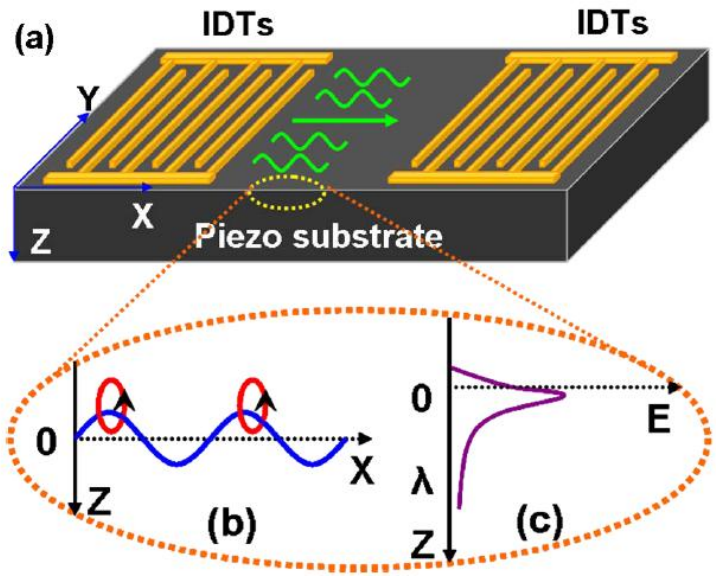

Figure 5.1.1. **Schematic of SAW**: (A) Shows parallel IDT setup with one IDTs generating SAW. (B) Localized drawing of SAW propagation on the surface. Also showing the elliptical path of a material point. (C) Energy of SAW in the z-direction. Much of the energy is near the surface. Source: From ref. 28

On the piezoelectric substrate, a SAW can propagate freely with little attenuation, as is characteristic of a sound wave on a free surface. The SAW velocity depends on the substrate, specifically the crystal orientation. In this setup 128º Y-X cut $LiNbO_3$ was used and the SAW velocity on this substrate is 3994 m/s [27]. When the SAW, encounters an obstruction, for example a microfluidic channel filled with incompressible liquid, the wave propagation becomes attenuated as there is a mismatch in the propagation velocity between the mediums and leakage waves are formed. A schematic of this proposed action can be seen in Figure 5.1.2. An intuitive understanding can be achieved if sound is considered to be a flow of wave energy and as the flow is interrupted by an object, the sound generates a force to push the object in the direction of flow propagation. Another explanation for the attenuation is that energy from the SAW is effectively transferred to the liquid medium. As SAW encounters the liquid medium it generates

pressure fluctuations, at an angle, see equation 5.1.1, determined by Snell's Law (see equation 5.1.1), which impart a force on the liquid molecules and anything in the medium[23].

$$\theta = arcsin\frac{v_{liquid}}{v_{substrate}} \tag{5.1.1}$$

Due to the wave attenuation, there develops a high pressure area, where the SAW first encounters the medium because more energy is transferred to the medium and low pressure area at the far end of the channel farther away from the SAW generation, because the attenuated wave cannot transfer as much energy to the medium. This pressure gradient leads to the formation of a re-circulatory flow in the channel. This re-circulatory flow is termed acoustic streaming.

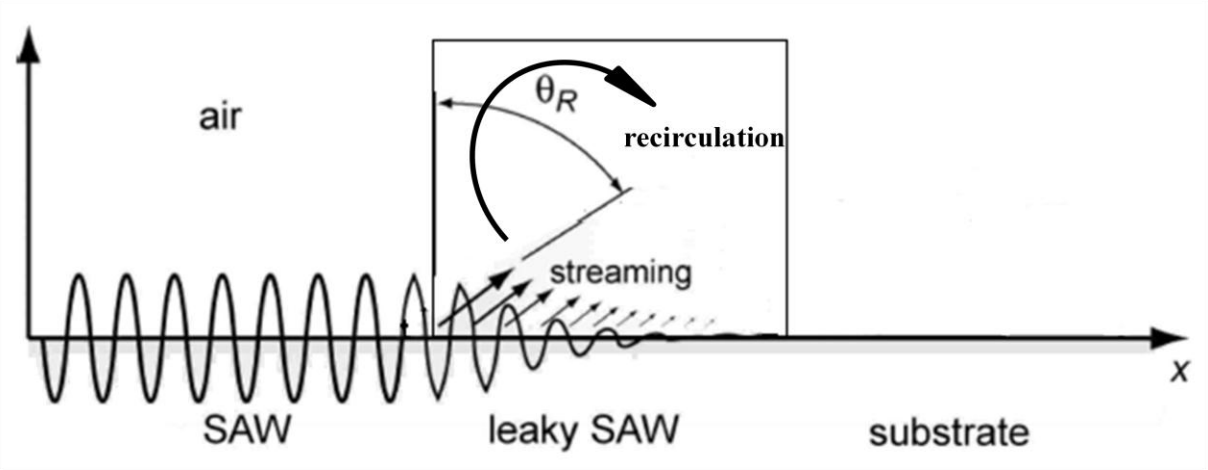

Figure 5.1.2: **Generation of acoustic streaming**: The image demonstrates SAW on the substrate, and as it encounters the liquid medium it generates leakage waves at an angle θ, determined by Snell's law. The attenuated SAW results in acoustic streaming and recirculating flow. Source: Adapted from ref. 23.

The acoustic streaming flow and the radiation pressures generated by the attenuated SAW as it propagates through the channel is what likely causes the particles in the channel to be displaced from one streamline to the next. Much theoretical work has been done to understand these phenomena, because of their potential applications at the interface of fluid dynamics and

acoustics [29, 30]. However, these effects exhibit non-linear properties, are usually dependent on second order terms, and are influenced by various parameters, so these phenomena are not completely understood. A common approach, considered in detail by Nyborg, to understand these phenomena is to start with the Navier-Stokes equation and continuity:

$$\nabla \cdot V = 0 \tag{5.1.1}$$

$$\rho \frac{\partial V}{\partial t} + \rho(V \cdot \nabla)V - \mu \nabla^2 V = -\nabla P + \rho F \tag{5.1.2}$$

Where V is the velocity field, ρ is density of the fluid, μ is viscosity of the fluid, P is pressure and F is the force in the system, in this case acoustic force. Nyborg after making simplifying assumptions about the flow field and applying knowledge of acoustics and how it couples with the fluid system arrived at the following equations, considered to be the governing equations of acoustic streaming of Nyborg's theory [27, 31]:

$$\mu \nabla^2 v_2 - \nabla p_2 = F \tag{5.1.3}$$

$$F = \rho_0 \langle (v_1 \cdot \nabla) v_1 + v_1 (\nabla \cdot v_1) \rangle \tag{5.1.4}$$

Where μ is the shear viscosity of the fluid, v_1 is the acoustic velocity field, v_2 is acoustic streaming velocity, p_2 is the steady state pressure, ρ_0 is the density under thermal equilibrium and F is the acoustic force in the system. The angled brackets denote the time average of the time dependent field. After simplifying assumptions, it was concluded by Frommetl et al. that the force in equation 5.1.2 is proportional to sound intensity and thereby proportional to the applied power[31]. This agrees with the proportional relationship derived experimentally between displacement and applied power.

In order to specifically solve for the acoustic streaming velocities and forces, various equations and other factors including Navier-Stokes, continuity, compressibility, time dependent boundary conditions must be considered. Also effects of the inner boundary, SAW propagation and forces from the fluid back on to the substrate would alter the expected solution. After simplifying assumptions, acoustic streaming velocities can be calculated by iterating values of first order velocities, which depend on the wave number, amplitude and attenuation, into equation 5.1.4 to yield values of forces and then using that result to obtain second order velocities. Theoretical calculations done by Nyborg and Sankaranarayanan demonstrate the streaming velocities are proportional to the amplitude squared [27, 29]. The amplitude squared is also proportional to power, so the streaming velocities are proportional to the applied power. As the applied power is time independent, it can be concluded that displacement due to the acoustic streaming velocity should be proportional to the power.

The results indicate that applying power levels as low as -1 dBm yield a shift in particles of 4.61 micrometers, which would be sufficient to push particles across streamlines. In order to engineer an efficient design, the theoretical principles must be understood. The theoretical principles essentially suggest that applied power should proportionally increase the displacement, as the higher applied power will impart greater forces on the particles. The experimental results, shows this general trend. However other affects such as the wall deformation, which is not accounted for by the theories, may cause the lack of agreement between the theoretical and experimental observations.

In addition to the velocity field generated by acoustic streaming, the force imparted on suspended particles in a fluid medium by acoustic radiation pressures is also of interest. In a related work Nyborg also considered the forces imparted on sphere by acoustic radiation

pressures[32]. Nyborg assumed a particle of radius 'a' was suspended in fluid of negligible viscosity and developed a theory by starting with the second order time averaged potential ($\bar{V}$) and kinetic energies ($\bar{T}$). By correlating sound field and fluid properties and making assumptions, such as the density of the particle is equivalent to that of the fluid as is the case in many biological situations, Nyborg arrived at:

$$F = \varepsilon v \frac{\partial \overline{T_a}}{\partial x} - v \frac{\partial \bar{V}_a}{\partial x} \tag{5.1.5}$$

Where ε is (ρ-ρ_0) /ρ_0 where ρ and ρ_0 are the particle and fluid densities respectively, v is the volume of the sphere, $\overline{T_a}$ is the time averaged kinetic energy density and $\bar{V}_a$ is the time averaged potential energy density. Nyborg concluded that the force on a small sphere is much larger in a standing wave (formed by in phase waves propagating in opposite directions with same amplitude) than in a progressive wave of comparable amplitude because of the non-uniformity of amplitude (i.e. attenuation). The energy profiles are determined by the applied power levels, suggesting a relationship between applied power and particle displacement. These equations were theoretically derived; however in the setup for the experiments it is quite difficult to obtain values for potential and kinetic energies.

The approach used in this later theory proposes another mechanism for the particle displacement; this approach suggests the particles migrate to specified energy wells, which depend on the SAW and applied power. The difficulty in obtaining energy distribution makes it hard to experimentally verify the theory. This theory however suggests that the forces are also proportional to the particle density and volume. By using these properties to our advantage, an efficient SAW driven sorting system can be designed. For example power consumption can be decreased as forces are larger in larger particles, particles with greater volume.

5.2 Future work

Although the principle of using acoustic forces to push particle across streamlines to achieve sorting seems quite simple, understanding the principles behind this effect is quite difficult. In order to optimize this system, the working principles must be better understood. A parameter that needs to be improved is the channel bonding to the $LiNbO_3$ substrate. Current techniques sometimes yield channels with air pockets which can eventually lead to bubble formations in the channel, or worse such as leakage. Another area of optimization is to reduce power consumption and to more efficiently displace the particles. Currently the highest power used is 0.5 dBm or 1.12 mW, which corresponds to a power intensity of 4593 W m^{-2}. Other SAW devices have shown larger displacements with less power; however the flow rates in these devices are significantly slower.

As mentioned earlier the acoustic streaming imparts a force on the particles, in order to ensure cellular viability further studies must be conducted. Previously SAW devices, used to pattern cells and seed cells into a scaffold, have been shown to be gentle towards cells and the low power used does not affect cellular viability [22, 33]. It has been shown that cells are still viable with powers of up to 10^9 W m^{-2} in optical tweezers and 2000 to 6000 W m^{-2} in bulk acoustic wave devices [22]. Cell lysis, primarily blood cell lysis by shear forces, is of great concern in the development of artificial organs. In order to characterize the shear threshold of blood cells, experiments have been conducted using Couette flow (similar to laminar flow) viscometers at constant shear with varying exposure times. It has been demonstrated that red blood cells can experience shear stress levels of 425 Pa for 620 ms before significant lysis occurs[34]. Although no cellular experiments were conducted with the device, the power used by the device is less than that in other techniques and the shear forces should not exceed 425 Pa. The exposure time to the

acoustic forces in the device is also considerably less than 620 ms. Considering these factors cellular viability should likely not be an issue with the device.

If cellular viability is demonstrated the next step would be to integrate the device with the microfluidic flow cytometer platform. In order to do so considerations about the working area of the SAW as well as the velocity of the particles must be known. This would provide information about the spacing between particles. Also the time to detect the particle and confer the signal to the IDT must be considered in order to place the IDT far enough downstream to account for the signal delay.

VI. Conclusion

Microfluidics offers a unique platform and seems poised to reshape various scientific sectors. A potential application of this technology is to miniaturize analytical tools such as flow cytometers. In order to realize these devices, scientists have taken a piecewise approach; demonstrating individual components before integrating all off the parts. In this thesis, a technique to achieve cell sorting is explored. Several current techniques exist to sort particles in a microfluidic channel however each technique presents unique advantages and limitations. In this thesis surface acoustic wave driven particle sorting mechanism is examined as an alternative to the other demonstrated techniques due to its advantages such as simple fabrication, low power consumption and its ability to act on all types of particles. Standard surface micromachining techniques and soft lithography techniques were used to fabricate the microfluidic device. It was effectively demonstrated that a focused flow of 7.4 micrometer particles can be deflected across streamlines and sorted downstream. A displacement versus power relationship was also examined and it dictated that with increasing power the displacement increased. Acoustic theory supported the proportional relationship between displacement and power. It was also theorized that the particle displacement is caused by the phenomenon of acoustic streaming, and radiation pressure. In conclusion, a SAW driven particle sorting mechanism was effectively demonstrated. More work is needed to optimize the system. Once optimized, the system can be integrated into a flow cytometer platform to achieve a fully integrated microfluidic flow cytometer.

VII. References

1. Feynman, R.P., *There's Plenty of Room at the Bottom.* Journal of Microelectromechanical Systems, 1992. **1**: p. 7.
2. Development, Y., *Preliminary Top 30 worldwide MEMS manufacturers*. 2008, I-Micronews.
3. *BioMEMS 2008 How Microsystems and Semiconductor Industries make money out of the Life Science market?* 2008, Yole Development.
4. Whitesides, G.M., *The origins and the future of microfluidics.* Nature, 2006. **442**(7101): p. 368-373.
5. Saliterman, S., *Fundamentals of BioMEMS and Medical Microdevices*. 2006: SPIE Publications.
6. Ateya, D.A., et al., *The good, the bad, and the tiny: a review of microflow cytometry.* Anal Bioanal Chem, 2008. **391**(5): p. 1485-98.
7. Macey, M.G., *Flow Cytometry: Principles and Applications*. 2007: Humana Press.
8. Shapiro, H.M., *Multistation Multiparameter Flow-Cytometry - a Critical-Review and Rationale.* Cytometry, 1983. **3**(4): p. 227-243.
9. Toner, M. and D. Irimia, *BLOOD-ON-A-CHIP.* Annual Review of Biomedical Engineering, 2005. **7**: p. 77-103.
10. Dongeun Huh, W., Yoko Kamotani James B Grotberg and S. Takayama, *Microfluidics for flow cytometric analysis of cells and particles.* Physiological Measurement, 2005. **26**: p. r73-r98.
11. Chen, C.C., et al., *Design and operation of a microfluidic sorter for Drosophila embryos.* Sensors and Actuators B-Chemical, 2004. **102**(1): p. 59-66.
12. Chen-Yi Lee, Y.-H.L., Gwo-Bin Lee, *A droplet-based microfluidic system capable of droplet formation and manipulation.* Microfluidics and Nanofluidics, 2009. **6**(5): p. 11.
13. Dongeun Huh, J.H.B., Yibo Ling, Hsien-Hung Wei, Oliver D. Kripfgans, J. Brian Fowlkes, James B. Grotberg, and Shuichi Takayama, *A Gravity Driven Microfluidic Particle Sorting Device with Hydrodynamic Seperation Amplification.* Analytical Chemistry, 2007. **79**(4).
14. Pamme, N., *Magnetism and microfluidics.* LAB ON A CHIP, 2006. **6**(1): p. 24-38.
15. Pamme, N., *Continuous flow separations in microfluidic devices.* Lab on a Chip, 2007. **7**(12): p. 1644-1659.
16. Holmes, D., et al., *On-chip high-speed sorting of micron-sized particles for high-throughput analysis.* Nanobiotechnology, IEE Proceedings -, 2005. **152**(4): p. 129-135.
17. Wang, L., et al., *Dielectrophoresis switching with vertical sidewall electrodes for microfluidic flow cytometry.* LAB ON A CHIP, 2007. **7**(9): p. 1114-1120.
18. Fu, A.Y., et al., *A microfabricated fluorescence-activated cell sorter.* NATURE BIOTECHNOLOGY, 1999. **17**(11): p. 1109-1111.
19. Fu, L.M., et al., *Electrokinetically driven micro flow cytometers with integrated fiber optics for on-line cell/particle detection.* Analytica Chimica Acta, 2004. **507**(1): p. 163-169.
20. Applegate, R.W., et al., *Microfluidic sorting system based on optical waveguide integration and diode laser bar trapping.* LAB ON A CHIP, 2006. **6**(3): p. 422-426.

21. Wang, M.M., et al., *Microfluidic sorting of mammalian cells by optical force switching.* NATURE BIOTECHNOLOGY, 2005. **23**(1): p. 83-87.
22. Shi, J.J., et al., *Acoustic tweezers: patterning cells and microparticles using standing surface acoustic waves (SSAW).* LAB ON A CHIP, 2009. **9**(20): p. 2890-2895.
23. Yeo, L.Y. and J.R. Friend, *Ultrafast microfluidics using surface acoustic waves.* Biomicrofluidics, 2009. **3**(1)
24. Franke, T., et al., *Surface acoustic wave (SAW) directed droplet flow in microfluidics for PDMS devices.* LAB ON A CHIP, 2009. **9**(18): p. 2625-2627.
25. Mao, X.L., et al., Single-layer planar on-chip flow cytometer using microfluidic drifting based three-dimensional (3D) hydrodynamic focusing. LAB ON A CHIP, 2009. 9(11): p. 1583-1589.
26. Mao, X.L., J.R. Waldeisen, and T.J. Huang, "Microfluidic drifting" - implementing three-dimensional hydrodynamic focusing with a single-layer planar microfluidic device. LAB ON A CHIP, 2007. 7(10): p. 1260-1262.
27. Sankaranarayanan, S.K.R.S. and V.R. Bhethanabotla, Design of efficient focused surface acoustic wave devices for potential microfluidic applications. Journal of Applied Physics, 2008. 103(6): p. -.
28. Shi, J., et al., Surface Acoustic Wave (SAW) induced patterning of micro Beads in microfluidic channels, 21st IEEE International Conference on Micro Electro Mechanical Systems (MEMS 2008), Tucson, Arizona, January 13-17, pp. 26-29, 2008
29. Nyborg, W.L., Acoustic Streaming Due to Attenuated Plane Waves. Journal of the Acoustical Society of America, 1953. 25(1): p. 68-75.
30. Lighthill, J., Acoustic Streaming. Journal of Sound and Vibration, 1978. 61(3): p. 391-418.
31. Frommelt, T., et al., Flow patterns and transport in Rayleigh surface acoustic wave streaming: Combined finite element method and raytracing numerics versus experiments. Ieee Transactions on Ultrasonics Ferroelectrics and Frequency Control, 2008. 55(10): p. 2298-2305.
32. Nyborg, W.L., Radiation Pressure on a Small Rigid Sphere. Journal of the Acoustical Society of America, 1967. 42(5): p. 947
33. Li, H.Y., et al., Effect of surface acoustic waves on the viability, proliferation and differentiation of primary osteoblast-like cells. Biomicrofluidics, 2009. 3(3)
34. Paul, R., et al., Shear stress related blood damage in laminar Couette flow. Artificial Organs, 2003. 27(6): p. 517-529.

Vita:

Karthik Pisupati

karthik.pisupati@psu.edu

Local Address:
348 Blue Course Dr.
Apt. 319A
State College, PA 16803
(610)-999-5025 (cell)

Permanent Address:
121 Barcladen Road
Bryn Mawr, PA 19010
(610)-581-4114

Education:

B.S. Bioengineering with a Chemical Engineering Option
Economics Minor
Schreyer's Honors Scholar
The Pennsylvania State University, University Park, PA
Graduation date: May 2010

Experience:

PSU BioNanoElectroMechanicalSystems (BioNEMS) Lab — Nov. 2008-Present

- Researching microfluidic flow cytometry
- Examined effects of Surface Acoustic Waves (SAW) on Liquid Crystals
- Wrote and edited manuscripts

Mashavu Project: Respiration Group Project Manager (Junior Design) — Spring 2009

- Managed and coordinated a team of 5 junior bioengineers
- Designed low cost spirometer to be implemented in Kenya

Biomedical Internship, Temple University, Philadelphia, PA — July-Aug. 2005

- Cultured growth of bacteria
- Performed Gel Electrophoresis
- Transformation (genetic engineering) of bacterial DNA

Achievements:

Dean's List: Fall 2006-Spring 2009
Spirit of BioE 401 award (best design process in junior design class)
Represented Engineering Design & Graphics 100 class in Annual Design Fair

Volunteer/Activities:

Second degree Black Belt in Tae Kwon Do
Volunteer Tae Kwon Do instructor

Computer Skills:

Programming in Java and Matlab
Familiar with Solid Works and COMSOL
Experience in Windows operating systems, and with Microsoft Office